

Three-dimensional quantitative structure–activity relationships study on HIV-1 reverse transcriptase inhibitors in the class of dipyridodiazepinone derivatives, using comparative molecular field analysis

Pornpan Pungpo and Supa Hannongbua

Department of Chemistry, Faculty of Science, Kasetsart University, Bangkok 10900, Thailand

A three-dimensional quantitative structure–activity relationships (3D QSAR) method, Comparative Molecular Field Analysis (CoMFA), was applied to a set of dipyridodiazepinone (nevirapine) derivatives active against wild-type (WT) and mutant-type (Y181C) HIV-1 reverse transcriptase. The starting geometry of dipyridodiazepinone was taken from X-ray crystallographic data. All 75 derivatives, divided into a training set of 53 compounds and a test set of 22 molecules, were then constructed and full geometrical optimizations were performed, based on a semiempirical molecular orbital method (AM1). CoMFA was used to discriminate between structural requirements for WT and Y181C inhibitory activities. The resulting CoMFA models yield satisfactory predictive ability regarding WT and Y181C inhibitions, with $r^2_{cv} = 0.624$ and 0.726 , respectively. CoMFA contour maps reveal that steric and electrostatic interactions corresponding to the WT inhibition amount to 58.5% and 41.5%, respectively, while steric and electrostatic effects have approximately equal contributions for the explanation of inhibitory activities against Y181C. The contour maps highlight different characteristics for different types of wild-type and mutant-type HIV-1 RT. In addition, these contour maps agree with experimental data for the binding topology. Consequently, the results obtained provide information for a

better understanding of the inhibitor–receptor interactions of dipyridodiazepinone analogs. © 2000 Elsevier Science Inc.

Keywords: HIV-1 RT, nevirapine, NNRTI, CoMFA, 3D-QSAR, quantum chemical calculations, molecular modeling

INTRODUCTION

11-Cyclopropyl-5,11-dihydro-4-methyl-6H-dipyrido[3,2-b:2',3'-e][1,4]diazepin-6-one or nevirapine (Figure 1), developed by Merluzzi et al.¹ is the first member of nonnucleoside reverse transcriptase inhibitors (NNRTIs) that has been approved for the treatment of human immunodeficiency virus (HIV-1) infections (Viramune®). This drug binds to an allosteric region at the protein and induces conformational changes, thereby inactivating the enzyme.^{2–5} Like other NNRTIs, however, nevirapine induces drug resistant variants of HIV-1, both in cell culture and in patients.^{6–8} The primary cause of this viral resistance to nevirapine and other NNRTIs is the mutation of the enzyme, which changes the shape of the pocket, where most of the reported NNRTIs are bound.⁹ Any small variation induced by a single point mutation can bring a significant impact on the sensitivity of the virus to members of NNRTIs, even for new drugs that have been recently introduced.¹⁰ Common features among these are mutations of Tyr181, which confer some degree of resistance to all of the nonnucleoside compounds,^{11–15} and of Tyr188, which also has significant effects on the binding of a variety of nonnucleoside drugs.¹⁶ In the case of nevirapine, the most commonly occur-

Color Plates for this article are on page 601.

Corresponding author: Supa Hannongbua, Kasetsart University, Faculty of Science, Department of Chemistry, Bangkok 10900, Thailand. Tel.: 066-2-942-8900; fax: 062-2-974-3955.

E-mail address: fscisph@ku.ac.th (S. Hannongbua)

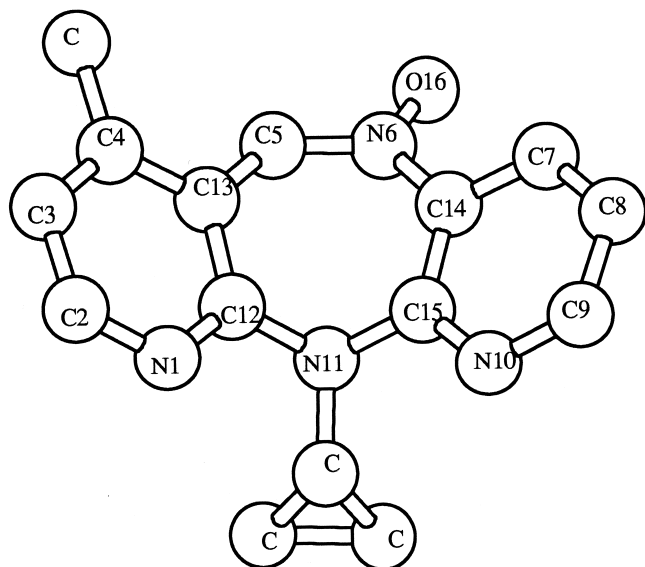


Figure 1. Structure of 11-cyclopropyl-5,11-dihydro-4-methyl-6H-dipyrido[3,2-b:2',3'-e] [1,4]diazepin-6-one and the atomic numbering as used in this study is indicated.

ring spontaneous mutation of Tyr181 is a replacement by cysteine.⁸ Only the crystal structure of the mutant enzyme (Y181C) and 8-Cl-TIBO has been reported already,¹³ but some publications dealt with the activity of nevirapine and its derivatives against both the wild-type and the Y181C mutant enzyme.^{17–19} In our previous investigations, we examined quantitative structure–activity relationships (QSAR) for NNRTIs to find common structural features among them.^{20–22} These studies provided information on electronic descriptors that affect inhibitor binding to reverse transcriptase. Furthermore, HIV-1 RT inhibitors in the class of 1-[(2-hydroxyethoxy)-methyl]-6-(phenylthio)thymine (HEPT) and benzodiazepinone analogs (TIBO) derivatives were investigated^{22,23} by means of three-dimensional quantitative structure–activity relationships (3D-QSAR) using Comparative Molecular Field Analysis (CoMFA).^{24–26} The results are successful in establishing the relationship between steric and electrostatic fields around molecules with their biological activities through contour maps. The structure of HEPT in the complex was also analyzed, based on molecular orbital calculations,^{27,28} to explain the intermolecular interactions between the inhibitor and the surrounding protein that determine the geometry of the inhibition complex. In the present study, CoMFA was applied to a class of dipyridodiazepinone derivatives to determine the different structural requirements concerning the WT and Y181C inhibition activities.

METHODOLOGY

Biological Data

The chemical structures of various dipyridodiazepinone derivatives and their inhibitory activities against both wild-type (WT RT) and mutant-type (Y181C) are reported elsewhere.^{17–19} All biological data are from the same laboratory and were estimated under the same experimental conditions. The potency has been defined as $\log(1/C)$, where C is the effective inhib-

itory concentration of compound required to achieve 50% (IC₅₀) protection of MT-4 cell against the cytopathic effect of HIV-1. A concentration range from C = 0.01 M up to C = 3.2 M was mentioned for the tests of biological activity. In most cases of weaker activity, concentration values higher than 1M were not given in the studies. Dipyridodiazepinone (compound 1, $\log(1/C) = 7.10$) is already used as a therapeutic agent (Viramune). Compounds 12 and 19 ($\log(1/C) = 8.00$) in Table 1 represent analogs with the highest activities, and compound 41 has the lowest activity ($\log(1/C) = 5.85$) in the studies^{17–19}. The range of biological activity in the data set is ~2 orders of magnitude in concentration, which is quite small compared with the typical range of 5–6 orders of magnitude for other SAR studies, but it is a consequence of the limited possibilities of the testing system. All compounds considered contain nitrogen atoms. Nevirapine exists in a nonprotonated form at physiological conditions.²⁹ Moreover, substituted aminopyridines show protonation constants at least 1 unit below the physiological pH value (pH ~8.0).³⁰ In the present analysis, based on these biological data, the structures of 53 dipyridodiazepinone compounds serve as a training set (Table 1). Twenty-two additional inhibitors were used as a test set to evaluate the predictive ability of the resulting models (Table 2).

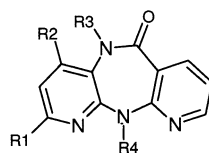
Molecular Modeling and Quantum Chemical Calculations

The starting geometry of dipyridodiazepinone is obtained from the crystallographic structure of the enzyme inhibitor complex.¹¹ Modification of substituents of all dipyridodiazepinones was performed by ALCHEMY 2000 program.³¹ The various dipyridodiazepinone derivatives differ mainly in the substituent R1. Therefore, a systematic analysis of this side chain substitution is necessary. The lowest energy conformer was examined using the systematic search technique available in SYBYL 6.4 program.³² All single bonds of the side chain were rotated with an increment of 2°. From this large number of conformations, the conformational minima were extracted in such a way that the nevirapine substructure was similar to the crystal structure. For the side chain, the lowest energy conformation was selected. No drastic conformational changes were observed during optimization procedure. Subsequently, full geometry optimization of all structures was carried out, based on AM1 semiempirical molecular orbital method implemented in the GAUSSIAN 94 program³³ on a DEC Alpha station (model 250-4266) (Digital Equipment Corp., Maynard, MA USA). Moreover, partial atomic charges required for the calculations of the electrostatic interactions were obtained by this method.

Alignment Rules and CoMFA Analysis

The alignment rule, i.e., the positioning of a molecular structure within a fixed lattice, is the most crucial element of the analysis. In this study, the field fit procedure in SYBYL 6.5³⁴ was adopted. The resemblance of a molecule to the template is considered in terms of both electrostatic and steric fields. Thus, the selected conformation is oriented to minimize the difference between its field values at the lattice points and those of the template field. An underlying assumption in QSAR analyses is that all molecules in the data set bind to the same receptor in a similar way. For these reasons, compounds 12 and 32 were retained as the template structure of the alignment rule for

Table 1. Structure of dipyridodiazepinone derivatives and experimental biological activities against both WT RT and Y181C RT



Cpds. No.	R1	R2	R3	R4	Experimental log (1/C)	
					WT RT	Y181C RT
1	H	CH ₃	H	C ₃ H ₅	7.10	5.58
2	H	CH ₃	H	C ₂ H ₅	7.40	5.74
3	H	H	CH ₃	C ₂ H ₅	6.89	5.66
4	CH ₃	CH ₃	H	C ₂ H ₅	7.70	6.00
5	CH ₂ CH ₃	H	CH ₃	C ₂ H ₅	6.92	5.92
6	CH(CH ₃) ₂	CH ₃	H	C ₂ H ₅	6.00	6.00
7	C(CH ₃) ₃	CH ₃	H	C ₂ H ₅	6.00	6.00
8	C=CHCOOCH ₃	H	CH ₃	C ₂ H ₅	6.74	6.17
9	C=CHCONH ₂	H	CH ₃	C ₂ H ₅	6.60	5.62
10	F	CH ₃	H	C ₂ H ₅	7.70	6.07
11	Cl	CH ₃	H	C ₃ H ₅	7.70	6.11
12	Cl	CH ₃	H	C ₂ H ₅	8.00	6.10
13	Cl	H	CH ₃	C ₃ H ₅	7.04	6.04
14	NH ₂	H	CH ₃	C ₂ H ₅	6.00	6.00
15	NH CH ₃	H	CH ₃	C ₂ H ₅	6.72	6.15
16	NH C ₂ H ₅	H	CH ₃	C ₂ H ₅	6.64	5.89
17	NHCH ₂ CH ₂ CH ₂ OH	CH ₃	H	C ₂ H ₅	7.04	6.00
18	N(CH ₃) ₂	H	CH ₃	C ₂ H ₅	7.15	6.11
19	N(CH ₃)CH ₂ CH ₂ OH	CH ₃	H	C ₂ H ₅	8.00	6.00
20	N-3,4-didehydropyrrolidinyl	H	CH ₃	C ₂ H ₅	7.52	6.19
21	N-piperidinyl	H	CH ₃	C ₂ H ₅	6.52	6.00
22	N-morpholinyl	H	CH ₃	C ₂ H ₅	6.40	6.00
23	N-thiomorpholinyl	CH ₃	H	C ₂ H ₅	6.82	6.00
24	N-pyrrolyl	H	CH ₃	C ₂ H ₅	7.04	6.68
25	OH	H	CH ₃	C ₂ H ₅	6.33	6.00
26	OCH ₃	H	CH ₃	C ₂ H ₅	7.40	6.22
27	OCH ₃	H	CH ₃	C ₃ H ₅	6.92	5.96
28	SCH ₃	CH ₃	H	C ₂ H ₅	7.70	6.00
29	2-furanyl	H	CH ₃	C ₂ H ₅	6.96	6.80
30	3-furanyl	H	CH ₃	C ₂ H ₅	7.40	6.96
31	2-pyrrolyl	H	CH ₃	C ₂ H ₅	7.15	7.15
32	3-pyrrolyl	H	CH ₃	C ₂ H ₅	7.52	7.40
33	3-pyrrolyl	H	CH ₃	C ₃ H ₅	7.30	7.22
34	2-thienyl	H	CH ₃	C ₂ H ₅	6.85	6.38
35	5-imidazolyl	H	CH ₃	C ₂ H ₅	6.89	6.72
36	3-pyrazolyl	H	CH ₃	C ₂ H ₅	6.41	6.54
37	4-pyrazolyl	H	CH ₃	C ₃ H ₅	7.22	7.20
38	phenyl	H	CH ₃	C ₂ H ₅	6.64	5.85
39	3-OCH ₃ -phenyl	H	CH ₃	C ₂ H ₅	6.82	6.68
40	3-NH ₂ -phenyl	H	CH ₃	C ₂ H ₅	7.15	6.25
41	4-OCH ₃ -phenyl	H	CH ₃	C ₂ H ₅	5.85	5.49
42	4-OH-phenyl	H	CH ₃	C ₂ H ₅	7.15	6.57
43	2-pyridyl	H	CH ₃	C ₂ H ₅	6.74	5.80
44	3-pyridyl	H	CH ₃	C ₃ H ₅	6.74	6.36
45	3-(6-OCH ₃ -pyridyl)	H	CH ₃	C ₂ H ₅	5.92	5.52
46	3-(6-OH-pyridyl)	H	CH ₃	C ₂ H ₅	5.96	6.00

(Continued)

Table 1. (Continued)

Cpds. No.	R1	R2	R3	R4	Experimental log (1/C)	
					WT RT	Y181C RT
47	3-(6-NH ₂ -pyridyl)	H	CH ₃	C ₂ H ₅	7.30	6.58
48	4-pyridyl	H	CH ₃	C ₃ H ₅	6.82	6.49
49	H	CH ₂ NHPh	H	C ₃ H ₅	7.22	5.86
50	H	CH ₂ O(Ph-p-NH ₂)	H	C ₃ H ₅	7.00	6.00
51	H	CH ₂ O(Ph-p-NHEt)	H	C ₃ H ₅	7.10	6.37
52	H	CH ₂ (Ph-o-OH)	H	C ₃ H ₅	6.72	5.95
53	OH	CH ₂ OOCH ₂ Ph	H	C ₂ H ₅	6.96	5.97

wild-type and mutant HIV-1 RT inhibitors, respectively. The electrostatic and the steric fields were computed using the Tripos force field. A three-dimensional cubic lattice, with 2 Å grid spacing, was generated automatically around these molecules, and it was ensured that the grid extended the molecular dimensions by 4 Å in all directions. In this study, three different atoms, sp³ carbon atom with +1 charge (default probe atom in SYBYL), sp³ oxygen atom with -1 charge and H atom with +1 charge served as probe atoms. The steric and electrostatic interactions are usually calculated by using sp³ C with +1 charge and H atom with +1 charge, respectively. In our study, sp³ O with -1 charge was included as another type of probe atom to extract additional information about both steric and electrostatic interactions. The probe atoms were placed at each lattice point and their steric and electrostatic interactions with each atom in the molecule were all computed with CoMFA standard scaling and then compiled in a CoMFA QSAR table. The minimum-sigma value was set to 2.0 kcal/mol to speed up the analysis and reduce the amount of noise. The energy cutoff values of 30 kcal/mol were selected for both electrostatic and steric field. Then, a partial least squares technique (PLS) was employed to derive a 3D-QSAR model expressing the correlation between the steric and the electrostatic properties and the inhibitory activities. The orthogonal latent variables were extracted by the NIPALS-algorithm³⁵ and subjected to full cross-validation (leave-one-out method). The analyses were carried out with a maximum of ten components, and subsequently, using the number of component (noc) at which the difference in the r^2_{cv} value to the next one was less than 0.05.³⁶ Consequently, a non cross-validated analysis was performed using the optimal number of components previously identified and was then employed to analyze the CoMFA results.

Predictive Ability

Q^2 or r^2_{cv} values were used to evaluate the overall predictive ability of the model. r^2_{cv} is calculated according to the following equation:

$$r^2_{cv} = (SSY - PRESS)/SSY$$

where SSY represents the variance of the biological activities of molecule around the mean value and PRESS is the prediction error sum of squares derived from the leave-one-out method. The uncertainty of the prediction is defined as

$$SPRESS = [PRESS/(n - k - 1)]^{1/2},$$

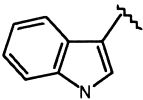
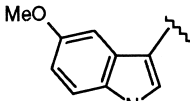
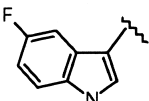
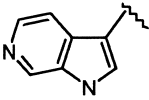
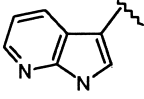
where k is the number of variables in the model and n is the number of compounds used in the study.

RESULTS AND DISCUSSION

CoMFA Models for WT-RT Inhibition

At first, the influence of the probe atoms was investigated, since CoMFA results depend on the interaction energy between these probe atoms and the molecules. All models obtained from the analyses include steric and electrostatic field contributions. In addition, separated analyses of steric or electrostatic fields only were also considered. The statistical parameters of the obtained correlation models are summarized in Tables 3–5. CoMFA with default setting probe atom, sp³ C(+1), produced a model with a low predictive ability, $r^2_{cv} = 0.029$ (model 1), as shown in Table 3. The low value of the noc of 1 is unusual. While other types of probe atoms, i.e., sp³ O (-1) and H (+1) yield better r^2_{cv} values (model 2, $r^2_{cv} = 0.148$ and model 3, $r^2_{cv} = 0.207$, respectively). However, this predictive power is rather low and some compounds are significantly out of line. The maximum outlier of each CoMFA models is also presented in Table 3. As compound 47 is found to be a maximum outlier of the best model, model 3, consequently, elimination of this compound from the CoMFA analysis yields model 4. Interestingly, the predictive ability of this model is drastically increased ($r^2_{cv} = 0.547$). However, another residual is still in the same range of compound 47. The consecutive outlier, compound 4, was removed resulting in model 5. Therefore, the final model is satisfied in both predictive ability ($r^2_{cv} = 0.624$) and the residual value of maximum outlier. The reason for the difference appeared in connection with outliers might be explained that these compounds adopt a different binding conformation at the receptor binding site. This statement is confirmed by the fact that as the maximum outlier, compound 47, has a much lower lipophilicity value, compared with the other two similar structures (compounds 45 and 46). The lipophilicity values of compounds 45, 46, and 47 are 2.81, 2.78, and 2.28, respectively. This evidence is also found in the similarity between compounds 4 and 2. Compound 4 is considered as an outlier with the logP value of 1.88. This value is much different than that of compound 2, which presents the lower lipophilicity, logP value of 1.37. Based on above results, the H probe atom was chosen for further studies on the effect of lattice spacing. The results of grid-CoMFA analysis, summarized in Table 4, indicated that 2 Å grid spacing was a good choice for

Table 2. Structure and predicted log (1/C) WT and Y181C HIV-1 RT inhibitory affinities of the tested dipyrrodiadiazepinone compounds

Cpds. No.	R1	R2	R3	R4	WT RT			Y181C RT		
					Expt. log (1/C)	Cal. log (1/C) ^a	Residual	Expt. log (1/C)	Cal. log (1/C) ^b	Residual
T1 ^c	CH ₃	CH ₃	H	C ₃ H ₅	7.15	7.10	0.05	5.92	5.91	0.01
T2 ^c	CH ₃	H	CH ₃	C ₂ H ₅	7.04	6.86	0.19	5.77	5.70	0.07
T3 ^c	C ₂ H	H	CH ₃	C ₂ H ₅	6.85	6.34	0.52	6.38	6.25	0.13
T4 ^c	Cl	H	CH ₃	C ₂ H ₅	7.10	6.92	0.17	6.68	5.93	0.75
T5 ^c	Br	H	CH ₃	C ₃ H ₅	7.52	6.89	0.63	5.68	5.78	-0.10
T6 ^c	NHCH ₂ CH ₂ OH	CH ₃	H	C ₂ H ₅	7.04	7.29	-0.25	6.00	5.67	0.33
T7 ^c	NHCH ₂ CH ₂ CH ₂ OH	CH ₃	H	C ₂ H ₅	7.04	7.61	-0.57	6.00	5.82	0.18
T8 ^c	N-pyrazolyl	H	CH ₃	C ₂ H ₅	6.51	6.81	-0.30	6.25	6.55	-0.29
T9 ^c	3-thienyl	H	CH ₃	C ₂ H ₅	7.00	6.99	0.01	6.52	6.48	0.04
T10 ^c	2-imidazolyl	H	CH ₃	C ₂ H ₅	5.43	6.34	-0.91	6.13	6.14	-0.01
T11 ^c	4-pyrazolyl	H	CH ₃	C ₂ H ₅	7.70	6.93	0.77	7.22	6.77	0.45
T12 ^c	2-OCH ₃ -phenyl	H	CH ₃	C ₂ H ₅	6.09	5.94	0.15	5.60	5.41	0.19
T13 ^c	3-OH-phenyl	H	CH ₃	C ₂ H ₅	7.00	7.25	-0.26	6.74	6.07	0.67
T14 ^c	4-NH ₂ -phenyl	H	CH ₃	C ₂ H ₅	7.40	7.25	0.15	6.92	6.58	0.34
T15 ^d	H	CH ₂ OPh	H	C ₃ H ₅	6.92	6.61	0.31	5.59	5.94	-0.35
T16 ^d	OH	CH ₂ Ph	H	C ₂ H ₅	6.47	7.32	-0.85	5.89	6.01	-0.13
T17 ^d	Ph-m-OMe	CHO	H	C ₂ H ₅	6.48	7.25	-0.77	6.38	6.44	-0.07
T18 ^e		H	CH ₃	C ₂ H ₅	7.55	6.84	0.71	7.55	7.50	0.05
T19 ^e		H	CH ₃	C ₂ H ₅	6.70	6.67	0.03	6.64	6.32	0.31
T20 ^e		H	CH ₃	C ₂ H ₅	6.15	6.62	-0.47	6.25	5.98	0.27
T21 ^e		H	CH ₃	C ₂ H ₅	7.36	6.67	0.69	7.01	6.69	0.32
T22 ^e		H	CH ₃	C ₂ H ₅	6.68	6.45	0.23	6.70	6.92	-0.23

^a Calculated by CoMFA model 5.

^b Calculated by CoMFA model 11.

^c Reference 17.

^d Reference 18.

^e Reference 19.

this set of molecule. A decrease in grid spacing increases the number of probe atoms in a region. However, it generates more noise in PLS analysis and leads to a worse r^2_{cv} value in this case. Apparently, model 5, obtained from including both steric and electrostatic fields in the analysis, shows the best predictive ability QSAR model with $r^2_{cv} = 0.624$, $s\text{-press} = 0.354$,

and $\text{noc} = 10$, which is abnormally high. Steric and electrostatic contributions of this model are 58.5% and 41.5%, respectively. Models using steric or electrostatic interaction only result in worse values of the predictive ability as shown in Table 3. Both steric and electrostatic interactions therefore play an important role in WT HIV-1 RT inhibition. The statistical

Table 3. Summary of CoMFA models for WT HIV-1 RT inhibition with 53 dipyrindodiazepinone compounds at different probe atoms

Mode 1	Probe atom	Field type	noc	r^2_{cv}	s-press	r^{2a}	s	F	Outliers (residual)	Steric contribution ^b
1	sp ³ C(+1)	both	1	0.029	0.518	0.247	0.456	16.702	compound 14 (−0.961)	65.6
		st	3	0.160	0.491	0.657	0.314	31.250		
		el	1	0.025	0.519	0.252	0.454	17.208		
2	sp ³ O(−1)	both	4	0.148	0.500	0.789	0.249	44.964	compound 47 (0.523)	62.2
		st	5	0.280	0.464	0.822	0.231	43.550		
		el	1	0.025	0.519	0.252	0.454	17.203		
3	H(+1)	both	4	0.207	0.482	0.808	0.237	50.620	compound 47 (0.581)	57.7
		st	9	0.354	0.460	0.957	0.120	93.810		
		el	1	0.025	0.519	0.252	0.454	17.203		
4 ^c	H(+1)	both	10	0.547	0.393	0.985	0.071	270.140	compound 4 (0.562)	57.8
		st	4	0.432	0.410	0.801	0.243	47.156		
		el	7	0.185	0.508	0.859	0.211	38.445		
5 ^d	H(+1)	both	10	0.624	0.354	0.989	0.062	348.133	compound 12 (0.152)	58.5
		st	10	0.528	0.597	0.967	0.104	119.015		
		el	7	0.233	0.488	0.859	0.178	54.075		

^a Conventional r^2 .^b Steric contribution in %.^c Elimination of compound 47 (remaining 52 compounds in the training set).^d Elimination of compound 47 and 4 (remaining 51 compounds in the training set).

characteristics obtained are that the conventional r^2 is 0.989, the standard error of estimate is 0.062, F is equal to 348.133 and the probability (P) to obtain this value of F if r^2 were actually zero (probability of $r^2 = 0$) is lower than 0.001. The experimental and the calculated affinities of model 5 derived from non-cross-validated analysis are plotted in Figure 2.

CoMFA Models for Y181C Inhibition

In further analyses, the CoMFA results with respect to Y181C inhibition were investigated. The statistics of the CoMFA models developed by different probe atoms are summarized in Table 5. For the default CoMFA setting, sp³C(+1), a r^2_{cv} value of 0.587 could be derived (model 6). Other probe atoms, sp³O(−1) and H(+1), yielded in worse predictive models (model 7, $r^2_{cv} = 0.506$ and model 8, $r^2_{cv} = 0.500$, respectively). Inspections of outliers obtained from CoMFA models were done and the maximum residual value is also presented in Table 5. A maximum outlier, compound 36, was found and elimination of this compound yielded a better model (model 9).

Nevertheless, other residual values are still in the same range as those derived from compound 36. Consequently, these consecutive outliers, compounds 38 and 43, were removed (models 10 and 11, respectively). Interestingly, as compound 43 was removed from CoMFA analysis, the quality of the model was increased to a high extent (model 10, $r^2_{cv} = 0.662$ and model 11, $r^2_{cv} = 0.726$). Finally, model 11 is satisfied in both predictive ability and maximum outlier. Based on outlier analysis, compounds 36 is found to be a maximum outlier in this set of mutant-type RT inhibitors. The consideration on the free rotatable pyrazolyl ring of R1 substituent of compounds 36 and 37 suggested that this might cause the different binding with the receptor and bring to different inhibitory affinity of both similar compounds. The same occurred to compound 43, compared with compound 44, where the 2-pyridyl substituent may not orient suitably to interact with the receptor that causes lower inhibition. The effect of grid spacing on CoMFA results was also studied. The r^2_{cv} indicated that grid spacing set to 2 Å was suitable for this data set as reported in Table 4. The reason

Table 4. The statistic results within lattice grid space by 1 Å and 2 Å for WT and Y181C HIV-1 RT inhibition

Type of HIV-1 RT	Probe atom	Grid (Å)	noc	r^2_{cv}	s-press	r^{2a}	s	F	Steric contribution ^b
WT HIV-1 RT	H (+1)	1	7	0.523	0.385	0.972	0.093	212.838	59.1
		2	10	0.624	0.354	0.989	0.062	348.133	58.5
Y181C HIV-1 RT	sp ³ C(+1.0)	1	9	0.658	0.293	0.991	0.048	474.071	49.6
		2	9	0.726	0.262	0.989	0.059	316.470	45.2

^a Conventional r^2 .^b Steric contribution in %.

Table 5. Summary of CoMFA models for Y181C HIV-1 RT inhibition with 53 dipyrindodiazepinone compounds at different probe atoms

Model	Probe atom	Field type	noc	r^2_{cv}	s-press	r^{2a}	s	F	Outliers (residual)	Steric contribution ^b
6	sp ³ C(+1)	both	8	0.587	0.313	0.968	0.087	167.287	compound 36 (0.151)	45.4
		st	3	0.301	0.386	0.942	0.120	68.131		
		el	4	0.407	0.359	0.791	0.213	45.458		
7	sp ³ O(-1)	both	5	0.506	0.332	0.928	0.128	99.462	compound 24 (0.256)	50.4
		st	4	0.319	0.385	0.759	0.229	34.759		
		el	4	0.407	0.359	0.791	0.213	45.458		
8	H(+1)	both	4	0.500	0.330	0.886	0.158	93.298	compound 42 (0.356)	47.5
		st	4	0.371	0.370	0.793	0.212	49.942		
		el	4	0.407	0.359	0.791	0.213	45.458		
9 ^c	sp ³ C(+1.0)	both	8	0.631	0.298	0.976	0.076	216.705	compound 38 (-0.151)	46.7
		st	3	0.292	0.406	0.675	0.264	33.268		
		el	4	0.392	0.366	0.789	0.215	44.013		
10 ^d	sp ³ C(+1.0)	both	8	0.662	0.287	0.071	0.979	245.70	compound 43 (0.109)	45.3
		st	3	0.287	0.394	0.679	0.264	33.074		
		el	4	0.388	0.369	0.790	0.216	43.253		
11 ^e	sp ³ C(+1.0)	both	9	0.726	0.262	0.989	0.059	316.470	compound 32 (0.120)	46.8
		st	3	0.322	0.385	0.705	0.254	36.605		
		el	4	0.436	0.359	0.808	0.207	47.280		

^a Conventional r^2 .^b Steric contribution in %.^c Elimination of compound 36 (remaining 52 compounds in the training set).^d Elimination of compounds 36 and 38 (remaining 51 compounds in the training set).^e Elimination of compounds 36, 38, and 43 (remaining 50 compounds in the training set).

could be explained in the same manner as far as WT inhibition. Inspection of the best QSAR model (model 11) in the series of Y181C RT inhibition revealed that this model has 46.8% contribution from steric field and 53.2% contribution from electrostatic field, with the $r^2_{cv} = 0.726$, $s\text{-press} = 0.262$, and $noc = 9$. Both steric and electrostatic effects have approximately equal contributions for the explanation of the Y181C inhibitory activity. This is also supported by the predictive power of the CoMFA results obtained from separated fields. Using steric or electrostatic interaction energy only provides worse values for the predictive abilities. Regarding the other statistical results, the conventional r^2 value obtained by PLS for the final model is 0.989, the standard error of estimate is 0.262, F is equal to 316.470 and the probability (p) to obtain this value of F if r^2 is really zero (probability of $r^2 = 0$) is less than 0.001. The experimental and calculated affinities of model 11 are depicted in Figure 2.

Prediction for Compounds in the Test Set

As the CoMFA models 5 and 11 show the highest predictive power for WT and Y181C RT inhibition, respectively, both models were used to predict the inhibitory activities of the compounds in the test set. The comparison of the observed and the predicted inhibitory activities of 22 compounds by models 5 and 11 are given in Table 2. This table shows clearly the usefulness of the models for the prediction of the activities of the dipyrindodiazepinone derivatives that are not included in the training set. Model 11 can accurately predict the activities of compounds T1, T2, T5, T9, T10, T17, and T18.

Steric and Electrostatic Contributions

The steric and electrostatic contributions for all dipyrindodiazepinone compounds are presented in the contour plots given in Color Plate 1 and Color Plate 2 derived from WT and Y181C inhibition CoMFA models, respectively. To better understand the steric and electrostatic interactions between the enzyme and inhibitors, the amino acid residues surrounding the dipyrindodiazepinone compound in the binding pocket were merged into both figures. The green contours in the maps indicate favorable steric effects in these regions, i.e., incorporation of bulkier groups will enhance the inhibitory activity. On the other hand, yellow contours in the maps show that bulkier groups in these regions reduce the receptor binding affinity. Concerning CoMFA electrostatic fields, a lower electron density at the inhibitors near blue and red contours increases or decreases the affinity, respectively.

Steric and Electrostatic Contributions for WT-RT Inhibition

With respect to CoMFA contour maps obtained for WT RT inhibition, Color Plate 1 presents yellow contours around the R1 substituent on the tricyclic ring, especially a yellow one overlapping with the Tyr181 residue. These contours reveal a limitation to the size of the substituent tolerated at this position. This means that an increase of the aliphatic bulk of the side chain leads to a steric conflict and, therefore, diminished favorable interactions with the aromatic ring of Tyr181 are found. This steric constrain is apparent in comparing 2-alkyl

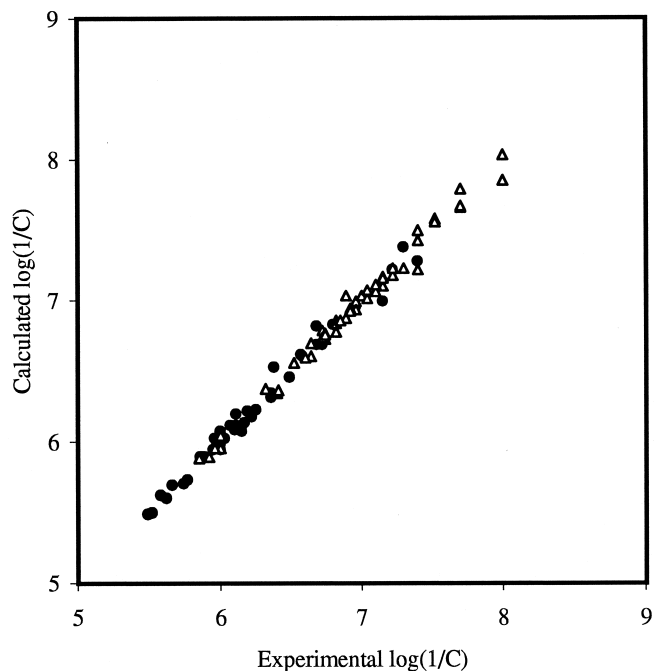


Figure 2. Plot of calculated versus experimental WT HIV-1 RT inhibitory affinities obtained from non-cross-validation of CoMFA model 5 for training set compounds, displayed in gray triangle and plot of calculated versus experimental Y181C HIV-1 RT inhibitory affinities obtained from non-cross-validation of CoMFA model 11 for training set compounds, displayed in black circle.

derivative (compound 4 and compounds 6–7), listed in Table 1, where a decrease in potency with the larger substituent is observed. The importance of the contact of the side chain R1 can also be seen by the crystallographic data of HIV-1 RT complexed with other NNRTIs.¹¹ We also found significant interactions of the inhibitors with the amino acid Tyr181. Additionally, a large red electrostatic contour region close to R1 position, partly overlapping the yellow contour, indicates that high negative charges in this area enhance the affinity. These results may be confirmed by the effect of the probe atom to the CoMFA model, as we found that the H(+1) probe atom provides the best CoMFA models (models 3–5). It can be summarized that not too bulky aliphatic groups and relatively high negative charges are required in this area. This suggestion is supported by experimental data, reported in Table 1, that the 2-F derivative (compound 10) and the 2-Cl derivatives (compounds 11–13) yield higher potency. In particular, compound 12 shows the highest potency for WT inhibition in this data set. A blue contour, close to the Glu138 residue, suggests that low electron density in this area will have a positive effect on the biological activity. The steric contour map also shows a green contour in the vicinity of Glu138. This reveals that the substituent at C2 position should have some orientation in this region as well because it should contain some atoms providing positive charge toward Glu138. This suggestion agrees with the trend observed experimentally that 2-aryl substitution yields effective inhibitors (compounds 30–33, Table 1).

Steric and Electrostatic Contributions for Y181C-RT Inhibition

Color Plate 2 shows the contributions of the steric and electrostatic fields to the Y181C RT inhibition. A large green contour corresponds to the location of the group attached to the C2 position on the tricyclic ring systems. However, the tolerated steric requirements of this region are highlighted by yellow contours located on each side of the favorable steric region. It is indicated that steric occupancy with bulky groups would increase the affinity, but the size of the substituent should not be too large. This evidence is supported by the effect of probe atom as sp^3C results the best CoMFA model (model 6). Effective inhibitors against WT RT will be less bulky substituents at C2 position such as compounds 1, 2, 4, and 10–13 have diminished activities against Y181C RT (see Table 1). Compounds 17–20, occupying the C2 position with too large substituents, display a significantly reduced potency against Y181C RT as well. In addition, a predominant feature of the electrostatic contour plot in this analysis is the presence of a large blue contour in the vicinity of the R1 substituent close to the Glu138 residue in the binding pocket. This contour indicates that positive charges in this region are more favorable for the binding affinity. As examples, compounds 30–33 with the aryl substitution at C2 should be mentioned. These compounds orient their pyrrolyl moieties into the green contour area; moreover, these groups are placed into the region indicated to be favorable to accommodate positive charges, yielding highly potent activity against Y181C RT. This can be supported by the comparison of compounds 17–20 with compounds 30–33. In particular, compound 32 shows the highest activity against Y181C RT. A blue contour is also presented in the CoMFA contour map obtained for WT inhibition in the approximately similar region. This may be the reason that compounds 30–33 show excellent inhibition against both WT and Y181C RT. In addition, there are favorable steric regions near the substituent attached to the C5 position which is close to Tyr188 and Trp229. This is also in agreement with the experimental results (Table 1), that the methyl substitution at this position confers better activity than that of an hydrogen atom. Based on the results, it could be confirmed that not only steric interactions contribute to the Y181C inhibitory activity, but also electrostatic interactions are important to explain the variance of the data. This is consistently found by Ren et. al.,¹¹ who stated that electrostatic interactions (between charges and by hydrogen bonding) contribute to the final strength of binding and may assist in the orientation of the compound, but specificity comes from the interactions with bulky hydrophobic residues. Using the crystal structures of nevirapine and its derivatives complexed with HIV-1 RT^{3,11}, it can be seen that there are contacts of the aromatic ring of Tyr181 with the bound inhibitor. Significant interactions between Glu138 and the NO_2 group attached to the C2 position of the tricyclic ring are also shown. Moreover, the favorable interactions between Tyr188 and Trp229 and the bound inhibitor are indicated. With regard to Y181C RT inhibition, substitution of Tyr181 by cysteine replaces the large aromatic side chain with a thiol group. It is clear that favorable interactions of the aromatic ring of Tyr181 and the bound inhibitor are eliminated. This mutation causes not only the necessity for more steric bulk of the side chain, but also the requirement of charges are changed. For these reasons, the affinities of some inhibitors are significantly

reduced. Based on our finding, it could be suggested that the pyrrolyl group is the best group for C2 substitution for the lacking aromatic amino acid at position 181. The loss of the aromatic ring system of this amino acid could be compensated by the presence of the pyrrolyl group. In addition, the charge distributions of this group are favorable for the association. These results show close agreement with our CoMFA models, which highlight the different structural requirements for WT and Y181C inhibitions of dipyrrodiazepinone derivatives.

CONCLUSIONS

3D QSAR models, using the CoMFA methodology, of dipyrrodiazepinone derivatives for the inhibition against both wild-type and Y181C RT were derived. CoMFA seems to be a helpful method to discriminate structural requirements between WT and Y181C inhibitory activities of these inhibitors. In this study, the QSAR models are reasonable based on both statistical significance and predictive ability. The CoMFA contour maps reveal that steric interactions play more significant role with respect to WT inhibition, while steric and electrostatic effects have approximately equal contributions toward explaining Y181C inhibitory activities. These contour maps show good consistency with inhibitor–receptor complexation derived by experimental data. Accordingly, these results lead to a better understanding of important drug–receptor interactions and structural requirements in the class of dipyrrodiazepinone compounds. Although we have not tested the compounds in a traditional Hansch-type QSAR analysis, 3D-QSAR information provides a helpful guideline to design and predict the affinity of novel compounds with enhanced WT and Y181C RT inhibitory activities prior to synthesis.

ACKNOWLEDGMENTS

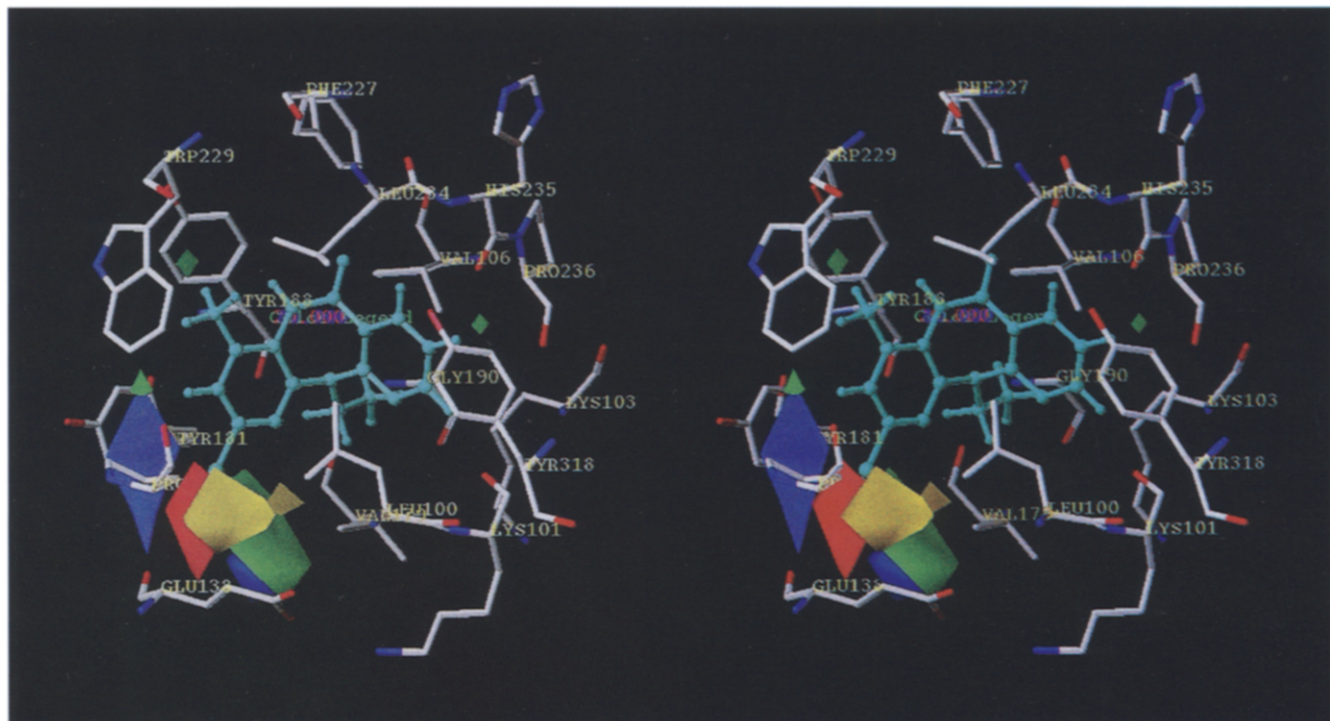
The authors would like to thank Professor P. Wolschann for critical comments on this paper, Dr. Surapoj Wongyai of Rungsit University for providing of SYBYL 6.4. The grants provided by the Thailand Research Funds (RSA4080022), KURDI, the Golden Jubilee Ph.D. project (3.C.KU/41/B.1), and the National Research Council of Thailand and Fonds zur Foerderung der Wissenschaftlichen Forschung (P12257-CHE) under the Austria–Thailand Cooperative Science Program (NRCT–FWF) are gratefully acknowledged. We thank the computing center of the University of Vienna for providing calculations in the cluster computer and to the high performance computing center of the National Electronics and Computer Technology of Thailand (NECTEC) for providing of SYBYL 6.5 calculations on SGI.

REFERENCES

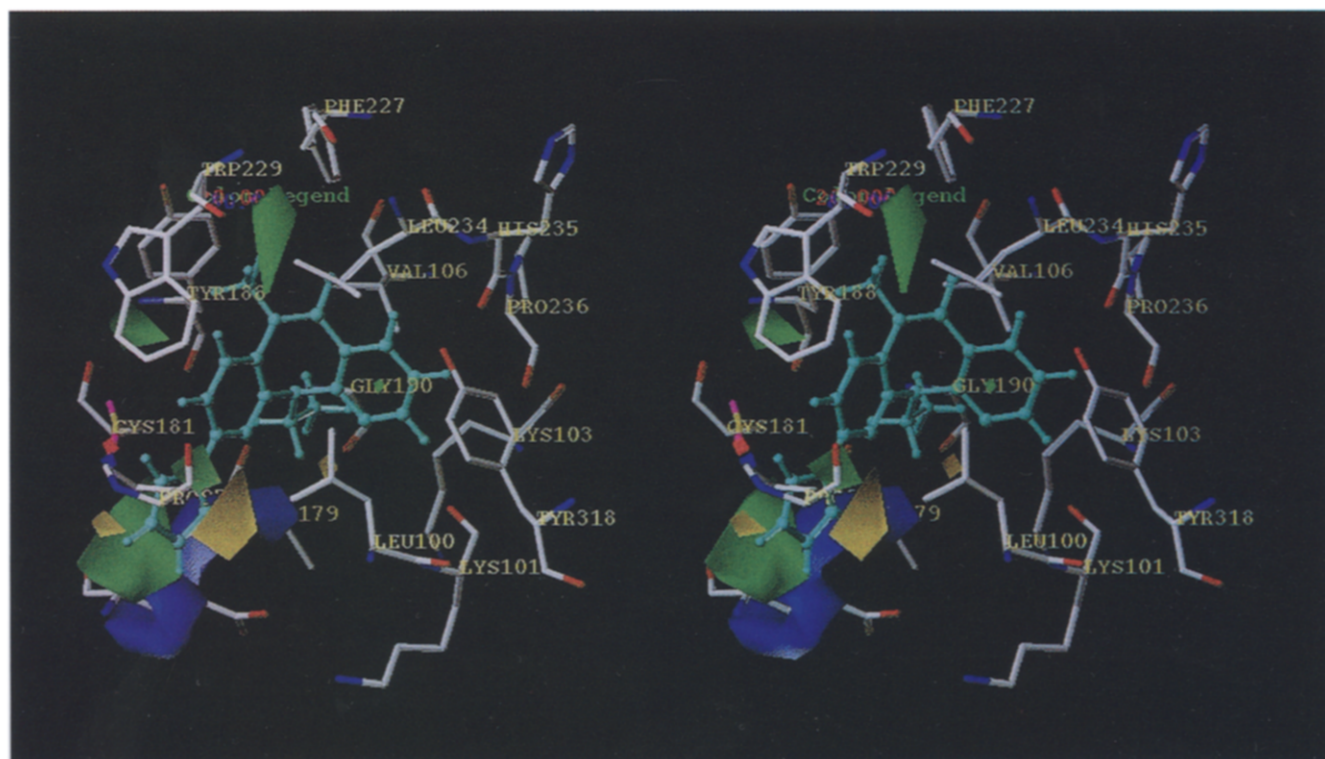
- 1 Merluzzi, V.J., Hargrave, K.D., Labadia, M.J., Grozinger, K., Skoog, M., Wu, J.C., Shinh, C., Shinh, C.-K., Eckner, K., Hattooy S., and Sullivan, L.L. Inhibition of HIV-1 replication by a nonnucleoside reverse transcriptase inhibitor. *Science*. 1990, **250**, 1411–1413
- 2 Kohlstaedt, L.A., Wang, J., Friedman, J.M., Rice, P.A., and Steitz, T. A. Crystal structure at 3.5 Å resolution of HIV-1 reverse transcriptase complexed with an inhibitor. *Science*. 1992, **256**, 1783–1790
- 3 Smerdon, S.J., Jager, J., Wang, J., Kohlstaedt, L.A., Friedman, J.M., Rice, P.A., and Steitz, T.A. Structure of the binding site for nonnucleoside inhibitors of the reverse transcriptase of human immunodeficiency virus type 1. *Proc. Natl. Acad. Sci. U.S.A.* 1994, **91**, 3911–3915
- 4 Wu, J.C., Warren, T.C., Adams, J., Proudfoot, J., Skiles, J., Raghavan, P., Perry, C., Potocki, I., Farina, P.R., and Grob, P.M. A novel dipyrrodiazepinone inhibitor of HIV-1 reverse transcriptase acts through a nonsubstrate binding site. *Biochemistry*. 1991, **30**, 2022–2026
- 5 Cohen, K.A., Hopkins, J., Ingraham, R.H., Pargellis, C., Wu, J.C., Palladino, D.E., Kinkade, P., Warren, T.C., Rogers, S., and Adams, J. Characterization of the binding site for nevirapine (BI-RG-587), a nonnucleoside inhibitor of human immunodeficiency virus type-1 reverse transcriptase. *J. Biol. Chem.* 1991, **266**, 14670–14674
- 6 Richman, D., Shih, C.K., Lowy, I., Rose, J., Prodanovich, P., Goff, S., and Griffin, J. Human immunodeficiency virus type 1 mutants resistant to nonnucleoside inhibitors of reverse transcriptase arise in tissue culture. *Proc. Natl. Acad. Sci. U.S.A.* 1991, **88**, 11241–11245
- 7 Mager, P.P. A Check on Rational Drug Design: Molecular Simulation of the Allosteric Inhibition of HIV-1 Reverse Transcriptase. *Med. Res. Rev.* 1997, **17**, 235–237
- 8 Balzarini, J., Karlsson, A., Sardana, V.V., Emini, E.A., Camarasa, M.J., and De Clercq, E. Human immunodeficiency virus 1 (HIV-1)-specific reverse transcriptase (RT) inhibitors may suppress the replication of specific drug-resistant (E138K) RT HIV-1 mutants or select for highly resistant (Y181C→C181I) RT HIV-1 mutants. *Proc. Natl. Acad. Sci. U.S.A.* 1994, **91**, 6599–6603
- 9 De Clercq, E. Non-nucleoside reverse transcriptase inhibitors (NNRTIs) for the treatment of human immunodeficiency virus type 1 (HIV-1) infections: strategies to overcome drug resistance development. *Med. Res. Rev.* 1996, **16**, 125–157
- 10 Hoegberg, M., Sahlberg, C., Engelhardt, P., Noreen, R., Kangasmetsae, J., Johansson, N.G., Oeberg, B., Vrang, L., Zhang, H., Sahlberg, B., Unge, T., Loevgren, S., Fridborg, K., and Baeckbro, K. Urea-PETT compounds as a new class of HIV-1 reverse transcriptase inhibitors. 3. Synthesis and further structure–activity relationships studies of PETT analogues. *J. Med. Chem.* 1999, **42**, 4150–4160
- 11 Ren, J., Esnouf, R., Garman, E., Somers, D., Ross, C., Kirby, I., Keeling, J., Darby, G., Jones, Y., Stuart, D., and Stammers, D. High resolution structures of HIV-1 RT from four RT-inhibitor complexes. *Nat. Struct. Biol.* 1995, **2**, 293–302
- 12 Ding, J., Das, K., Moereels, H., Koymans, L., Andries, K., Janssen, P.A., Hughes, S.H., and Arnold, E. Structure of HIV-1 RT/TIBO R 86183 complex reveals similarity in the binding of diverse nonnucleoside inhibitors. *Nat. Struct. Biol.* 1995, **2**, 407–415
- 13 Das, K., Ding, J., Hsiou, Y., Clark, A.D. Jr., Moereels, H., Koymans, L., Andries, K., Pauwels, R., Janssen, P.A., Boyer, P.L., Clark, P., Smith, R.H. Jr., Kroeger, Smith M.B., Michejda, C.J., Hughes, S.H., and Arnold, E. Crystal structures of 8-Cl and 9-Cl TIBO complexed with wild-type HIV-1 RT and 8-Cl TIBO complexed with the Tyr181Cys HIV-1 RT drug-resistant mutant. *J. Mol. Biol.* 1996, **264**, 1085–1100

- 14 Tantillo, C., Ding, J., Jacobo-Molina, A., Nanni, R.G., Boyer, P.L., Hughes, S.H., Pauwels, R., Andries, K., Janssen, P.A., and Arnold, E. Locations of anti-AIDS drug binding sites and resistance mutations in the three-dimensional structure of HIV-1 reverse transcriptase. Implications for mechanisms of drug inhibition and resistance. *J. Mol. Biol.* 1994, **243**, 369–387
- 15 Ding, J., Das, K., Tantillo, C., Zhang, W., Clark, A.D. Jr., Jessen, S., Lu, X., Hsiou, Y., Jacobo-Molina, A., and Andries, K. Structure of HIV-1 reverse transcriptase in a complex with the non-nucleoside inhibitor alpha-APA R 95845 at 2.8 Å resolution. *Structure*. 1995, **3**, 365–379
- 16 Hsiou, Y., Das, K., Ding, J., Clark Jr., A.D., Kleim, J., Roesner, M., Winkler, I., Riess, G., Hughes, S.H., and Arnold, E. The structure of Tyr188Leu mutant and wild-type HIV-1 reverse transcriptase complexed with the non-nucleoside inhibitor HBY 097:inhibitor flexibility is a useful design feature for reducing drug resistance. *J. Mol. Biol.* 1998, **284**, 313–323
- 17 Proudfoot, J.R., Hargrave, K.D., Kapadia, S.R., Patel, U.R., Grozinger, K.G., McNeil, D.W., Cullen, E., Cardozo, M., Tong, L., Kelly, T.A., Mauldin, S.C., Fuchs, V.U., Vitous, J., West, M., Klunder, J., Raghavan, P., Skiles, J.W., Mui, P., Rose, J., David, E., Richmond, D., Sullivan, J. L., Farina, V., Shih, C.K., Grob, P.M., and Adams, J. Novel non-nucleoside inhibitors of human immunodeficiency virus type 1 (HIV-1) reverse transcriptase. 4. 2-substituted dipyrindiazepinones as potent inhibitors of both wild-type and cysteine-181 reverse transcriptase enzyme. *J. Med. Chem.* 1995, **38**, 4830–4838
- 18 Kelly, T.A., Proudfoot, J.R., McNeil, D.W., Patel R.U.P., David, E., Hargrave, K.P., Peter M., Cardozo, M., Agarwal, A., and Adams, J. Novel non-nucleoside inhibitors of human immunodeficiency virus type 1 reverse transcriptase. 5. 4-substituted and 2,4-disubstituted analogs of nevirapine *J. Med. Chem.* 1995, **38**, 4839–4847
- 19 Kelly, T.A., McNeil, D.W., Rose, J.M., David, E., Shih, C.K., and Grob, P.M. Novel non-nucleoside inhibitors of human immunodeficiency virus type 1 reverse transcriptase. 6. 2-Indol-3-yl- and 2-azaindol-3-yl-dipyrindiazepinones. *J. Med. Chem.* 1997, **40**, 2430–2433
- 20 Hannongbua, S., Lawtrakul, L., and Limtrakul, J. Structure–activity correlation study of HIV-1 inhibitors: Electronic and molecular parameter, *J. Comp. Aided Mol. Des.* 1996, **10**, 145–152
- 21 Lawtrakul, L., and Hannongbua, S. Quantitative structure–activity relationships of HIV-1 RT inhibitors in the class of 1-[(2-Hydroxyethoxy)methyl]-5,6-substituted thymine [HEPT] analogues. *Sci. Pharm.* 1999, **67**, 43–56
- 22 Hannongbua, S., Pungpo, P., Limtrakul, J., and Wolschann, P. Quantitative structure–activity relationships and comparative molecular field analysis of the HIV-1 reverse transcriptase inhibitor of TIBO derivatives. *J. Comp. Aided Mol. Des.* 1999, **13**, 563–577
- 23 Hannongbua, S., Lawtrakul, L., Sottriffer, C.A., and Rode, B.M. Comparative molecular field analysis of the HIV-1 reverse transcriptase inhibitors in the class of 1-[(2-Hydroxyethoxy) -methyl]-6-(phenylthio)thymine. *Quant. Struct.-Act. Relat.* 1996, **15**, 389–394
- 24 Cramer, R.D., III, Patterson, D.E., and Bunce, J.D. Comparative molecular field analysis (CoMFA). 1. Effect of shape in binding of steroids to carrier proteins. *J. Am. Chem. Soc.* 1988, **110**, 5959–5967
- 25 Oprea, T.I., and Waller, C.L. Theoretical and practical aspects of three-dimensional quantitative structure–activity relationships. In: *Reviews in Computational Chemistry*, Lipkowitz, K.B., and Boyd, D.B., Eds., Wiley-VCH, New York, 1997, Vol. 11, pp. 127–182
- 26 Greco, G., Novellino, E., and Martin, Y.C. Approaches to three-dimensional quantitative structure–activity relationships. In: *Reviews in Computational Chemistry*, Lipkowitz, K.B., and Boyd, D.B., Eds., Wiley-VCH, New York, 1997, Vol. 11, pp. 183–240
- 27 Lawtrakul, L., Hannongbua, S., Beyer, A., Wolschann, P. Conformational study of the HIV-1 reverse transcriptase inhibitor 1-[(2-Hydroxyethoxy)methyl]-6-(phenylthio)thymine (HEPT). *Biol. Chem.* 1999, **380**, 265–267
- 28 Lawtrakul, L., Hannongbua, S., Beyer, A., and Wolschann, P. Molecular calculations on the conformation of the HIV-1 reverse transcriptase inhibitor 1-[(2-Hydroxyethoxy)methyl]-6-(phenylthio)thymine (HEPT). *Monatsch. Chem.* 1999, **130**, 1347–1363
- 29 <http://www.viramune.com/ProductInfo/FullPrescribingInfo.html#description>
- 30 CRC Handbook of Chemistry and Physics, 58th edition, CRC PRESS Inc., Cleveland, Ohio, 1977–1978, p. 148–149
- 31 Alchemy 2000, Tripos Associates Inc., St. Louis, MO, 1998
- 32 SYBYL 6.4, Tripos Associates Inc., 1699 South Hanley Road, Suite 303, St. Louis, Missouri 63144, USA
- 33 Frisch, M.J., Trucks, G.W., Schlegel, H.B., Gill, P.M.W., Johnson, B.G., Robb, M.A., Cheeseman, J.R., Keith, T., Petersson, G.A., Montgomery, J.A., Raghavachari, K., Al-Laham, M.A., Zakrzewski, V.G., Ortiz, J.V., Foresman, J.B., Peng, C.Y., Ayala, P.Y., Chen, W., Wong, M.W., Andres, J.L., Replogle, E.S., Gomperts, R., Martin, R.L., Fox, D.J., Binkley, J.S., Defrees, D.J., Baker, J., Stewart, J.P., Head-Gordon, M., Gonzales, C., and Pople, J.A. GAUSSIAN 94, Revision B.3, Gaussian, Inc., Pittsburgh PA, 1995
- 34 SYBYL 6.5, Tripos Associates Inc., 1699 South Hanley Road, Suite 303, St. Louis, Missouri, 63144, USA
- 35 Wold, S., Johansson, E., Cocchi, M., and Kubinyi, H. 3D QSAR in Design : Theory, Methods and Applications, Leiden, ESCOM 1993, pp. 523–549
- 36 SYBYL Molecular Modelling Software, version 6.3, SYBYL Ligand Base Design, Tripos Associates, Inc., St. Louis, Missouri 63144, USA, 1996, p. 229

Three-dimensional quantitative structure–activity relationships study on HIV-1 reverse transcriptase inhibitors in the class of dipyrindodiazepinone derivatives, using comparative molecular field analysis



Color Plate 1. Stereoview of CoMFA steric and electrostatic STDEV*COEFF contour plots from the analysis of the 3D-QSAR model 5 with non-cross-validation based on WT HIV-1 RT inhibition. Green contours refer to sterically favored regions; yellow contours indicate disfavored area. Blue contours refer to positive charge favoring areas; red contours indicate negative charge favoring areas. Compound 12 is displayed inside the fields as ball and stick presentation.



Color Plate 2. Stereoview of CoMFA steric and electrostatic STDEV*COEFF contour plots from the analysis of the 3D-QSAR model 12 with non-cross-validation based on Y181C HIV-1 RT inhibition. Green contours refer to sterically favored regions; yellow contours indicate disfavored area. Blue contours refer to positive charge favoring areas; red contours indicate negative charge favoring areas. Compound 32 is displayed inside the fields as ball and stick presentation.